Pergamon

Cement and Concrete Research, Vol. 28, No. 3, pp. 439–452, 1998

0008-8846/98 $19.00 + .00

PII S0008-8846(97)00275-5

APPLICATIONS OF STRESS CRACK WIDTH RELATIONSHIP IN PREDICTING THE FLEXURAL BEHAVIOR OF FIBRE-REINFORCED CONCRETE

J. Zhang[1] and H. Stang
Department of Sturctural Engineering and Materials, Technical University of Denmark, Building 118, DK-2800 Lyngby, Denmark

(Received July 28, 1997; in final form December 19, 1997)

ABSTRACT

A semi-analytical model for the flexure behaviour of fibre-reinforced concrete (FRC) materials has been presented based on the equilibrium of force in the critical cracked section. The model relies on the bridging law, the so-called stress-crack width relation, as the fundamental constitutive relationship in tension. A good agreement has been found between the model predictions and experimental results, as well as between finite element calculations in terms of load-crack mouth opening displacement (CMOD) and load-deflection diagrams. This model's results lead to the conclusion that the flexure performance of FRC materials is strongly influenced by the stress-crack width relationship. The optimum flexure behaviour of FRC materials optimizes the bond properties of aggregate/matrix and fibre/matrix interfaces. © *1998 Elsevier Science Ltd*

Introduction

The flexure behaviour of unreinforced cementitious composites as concrete and fibre-reinforced concrete (FRC) is important for many current applications such as overlays for highways, bridge decks, airport pavements, roofing tiles, and partition walls. Concrete is a relative brittle material. As a result, the mechanical behaviour of concrete structures is critically influenced by crack propagation. Therefore, many attempts have been made to apply the concepts of fracture mechanics to analyze the fracture process of concrete. Because of the heterogeneity of concrete that causes the formation of a fracture process zone in front of a crack, it is realized that linear elastic fracture mechanics is only applicable to large-scale initially cracked structures and ultrabrittle concrete (1,2). So it is necessary to apply nonlinear fracture mechanics to describe the fracture process in ordinary concrete structures, especially in fibre-reinforced concrete structures. Various models based on nonlinear fracture mechanics that describe the fracture process zone in front of a crack of unreinforced and reinforced concrete have been developed, such as (1) the fictitious crack model (FCM) proposed by Hillerborg et al. (1,2) and the crack band theory proposed by Bazant et al. (2). The FCM has

[1]To whom correspondence should be addressed.

been successfully used to describe tensile stress induced fracture behaviour in nonyielding materials like concrete, rock, etc. In recent years, few FCM-based analytical models for predicting the structural behaviour of concrete and FRC beams under monotonic bending load have been developed. Ulkjær et al. (3) developed an analytical model of plain concrete beam in bending based on plastic hinge analysis that assumes development of a fictitious crack in an elastic layer with a thickness proportional to the beam depth. A linear tension softening relation is assumed. Pedersen (4) developed a similar model for plain as well as FRC structures, beams, and pipes, in which a more accurate softening law, a power function proposed by Stang et al. (5), is adopted. Maalej et al. (6) developed an analytical model of FRC beam in flexure based on a fracture mechanics approach with a discrete crack assumption. Here the authors adopt the analytic softening relations presented by Maalej et al. (7) and Li (8). Recent theoretical study shows that the bridging law for the period of smaller crack width (less than 0.1 mm) can strongly affect structural behaviour such as bending, under monotonic and cyclic load (9,10). The experimental results on stress-crack width relation show that the power function cannot fit the experimental data very well for FRC when the crack width is less than 0.1 mm. A more accurate stress-crack width model for FRC is necessary in order to predict the structural performance of FRC structures.

The major objective of the present work is to build up a semi-analytical method for predicting the flexural behaviour of unreinforced concrete structures and FRC structures based on fracture mechanics approach. In this model, the bridging law, the so-called stress-crack width relationship is incorporated as integration form which can easily be replaced by the other bridging models for different kinds of FRC materials with different fibre types, volume concentration, and matrix properties. In this paper, a much more accurate stress-crack width relationship, a four-linear model based on the uniaxial tensile tests, is adopted and applied to two types of concrete reinforced with straight and hooked steel fibre, respectively. The complete theoretical load-deformation curves, in terms of load-deflection and load-crack mouth opening displacement (CMOD) diagrams, are obtained and compared with the experimental results as well as with the finite element calculations. The results are discussed and conclusions are drawn at end of the paper.

The Constitutive Law of Concrete and FRC

It is assumed that the concrete and FRC materials considered here are materials that essentially show a linear response in uniaxial tension up to peak load. After peak, one discrete crack is formed. It is furthermore assumed that the discrete crack formation is described by the stress-crack width ($\sigma - w$) relationship. Thus the following material parameters are fundamental in the constitutive relations of concrete and FRC in tension: the Young's modulus E, the tensile strength σ_t, and the stress-crack width ($\sigma - w$) relationship. It is assumed that the behaviour of concrete and FRC materials in compression is linear elastic, and the Young's modulus in compression is the same as in tension.

The stress-crack width relationship of FRC materials has been investigated both experimentally and theoretically during recent years. The experimental results show that the shape of stress-crack width curve of FRC materials is complex and greatly influenced by the type and amount of fibre used (11,12). A micromechanics-based model for the stress-crack width relationship of FRC materials has been developed by Li et al. (13), which makes it is possible to predict the bridging law of FRC materials with single or hybrid fibre systems.

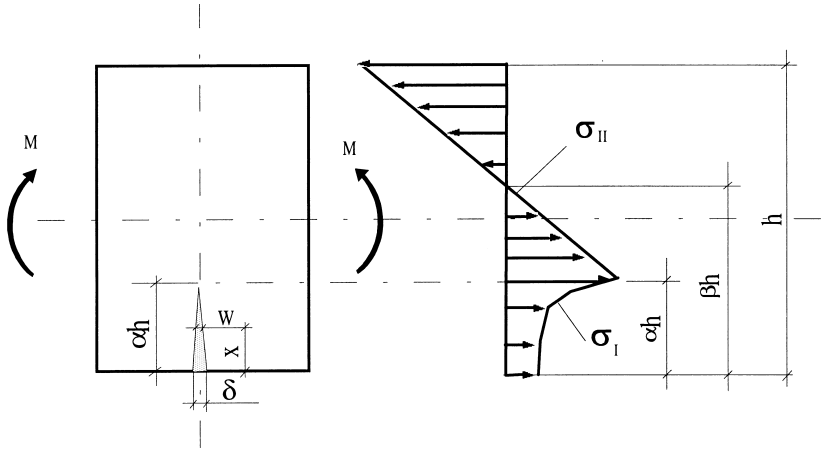

FIG. 1.
Distribution of normal stress in the cracked beam section.

Derivation of Model

Consider a short segment of a simple supported rectangular beam with width b, depth h, and span L that is subjected to an external bending moment M. The behaviour is assumed to be elastic until the maximum principal tensile stress reaches the tensile strength of material. After that it is assumed a single crack is formed with a maximum tensile strength at the crack tip. The moment corresponding to the initiation of the fictitious crack is the so-called first crack moment, M_{fc}, or first crack load, P_{fc}, when the moment is transformed into load. Thus the failure process of beam can be divided into two stages: 1) a linear elastic stage, and 2) a fictitious crack developing stage. The assumed stress distribution in the second stage is shown in Figure 1.

In the first stage, according to classical elastic theory, we have:

$$M_{fc} = \frac{2I}{h}\sigma_t = \frac{bh^2}{6}\sigma_t \tag{1}$$

where I is the moment of interia of beam and σ_t is the tensile strength of materials.

In the second stage, the crack length αh, $\alpha \epsilon [0,1]$, CMOD δ, and external moment M can be related through the fracture mechanics approach. First we assume that the crack has a linear profile, then:

$$w = \delta\left(1 - \frac{x}{\alpha h}\right) \tag{2}$$

where w is crack width at location x; see Figure 1. Next from the equilibrium conditions, we have:

$$\int_0^{\alpha h} \sigma_1(x) b dx + \int_{\alpha h}^{h} \sigma_{II}(x) b dx = 0 \tag{3}$$

$$\int_0^{\alpha h} \sigma_I(x)(h - x)bdx + \int_{\alpha h}^{h} \sigma_{II}(x)(h - x)bdx = M \tag{4}$$

where $M = PL/4$ for three-point bending case (P is external load) and $\sigma_I(x)$, and $\sigma_{II}(x)$ are the normal stress function in the cracked and uncracked parts, respectively. $\sigma_I(x)$ can be related with αh and δ through the stress-crack width relationship together with Eq. 2 as:

$$\sigma_I(x) = \sigma(w) = \sigma\left(\delta\left(1 - \frac{x}{\alpha h}\right)\right) \tag{5}$$

From the assumed stress distribution at uncracked part, $\sigma_{II}(x)$ can be related with αh, βh, and δ by:

$$\sigma_{II}(x) = \sigma_t\left(1 - \frac{x - \alpha h}{\beta h - \alpha h}\right) \tag{6}$$

where βh is the depth of tensile zone $\beta \epsilon [0,1]$. In order to obtain the complete solution of external load and CMOD for a given crack length, another relationship between them is necessary. Similar to Maalej et al. (6), the CMOD under bending load can be decomposed as:

$$\delta = \delta_M + \delta_{\sigma_1(x)} \tag{7}$$

where δ_M and $\delta_{\sigma I(x)}$ are the CMOD components caused by the external moment M and bridging stress $\sigma_I(x)$, respectively. $\delta_{\sigma I(x)}$ can be obtained through simplifying the $\sigma_I(x)$ as a cracked beam with crack length αh subjected to moment M' and axial stress σ'. Then:

$$\delta_{\sigma_I(x)} = \delta_{M'} + \delta_{\sigma'} \tag{8}$$

where M' and σ' are given by:

$$M' = \int_0^{\alpha h} b\sigma_I(x)\left(\frac{h}{2} - x\right)dx \tag{9}$$

$$\sigma' = \frac{1}{h}\int_0^{\alpha h} \sigma_I(x)dx. \tag{10}$$

According to Tada et al. (14), the total CMOD can be expressed as:

$$\delta = \frac{24\alpha}{bhE}\left[MV_1(\alpha) - M'V_2(\alpha)\right] - \frac{4\sigma'\alpha h}{E}V_3(\alpha) \tag{11}$$

where, under three-point bending load,

$$V_1(\alpha) = 0.33 - 1.42\alpha + 3.87\alpha^2 - 2.04\alpha^3 + \frac{0.66}{(1 - \alpha)^2}$$

$$V_2(\alpha) = 0.8 - 1.7\alpha + 2.4\alpha^2 + \frac{0.66}{(1 - \alpha)^2}$$

$$V_3(\alpha) = \frac{1.46 + 3.42\left(1 - \cos\frac{\pi\alpha}{2}\right)}{\left(\cos\frac{\pi\alpha}{2}\right)^2}$$

where $V_1(\alpha)$ is a slightly changed Tada's function after comparing with the authors' finite element implementation.

The determination of external moment and CMOD for a given crack length is performed according to the following algorithm. For a given crack length, αh, the external loading capacity, M, (which can easily be transformed into load capacity P according to a specific loading form) and corresponding CMOD, δ, are determined by solving nonlinear Eqs. 3, 4, and 11 through a simple bisection iteration scheme. For each guessed δ' and M a M' and σ' are determined from Eqs. 3 and 4 and Eqs. 9 and 10 using the numerical integration method. Then the calculated δ can be obtained from Eq. 11. The new guessed δ' will input until the equilibrium criterion is satisfied. Afterwards another crack length increment starts until the crack length reaches the prescribed end value.

Load-Deflection Curves

The deflection of a beam submitted to bending load and presenting a single crack in the central section can be estimated as follows. As an example, a three-point bending load case is considered here.

Before cracking, according to classical beam theory with the rectify on affect of shear stress (15), the central elastic deflection f_e is related to load P and span L as follows:

$$f_e = \frac{1}{48}\frac{PL^3}{EI}\left[1 + 2.85\left(\frac{h}{L}\right)^2 - 0.84\left(\frac{h}{L}\right)^3\right]. \tag{12}$$

After cracking, the total deflection f_t is assumed to be equal to the sum of two terms:

$$f_t = f_e + f_c \tag{13}$$

where f_c is additional deflection due to cracking. The cracking related deflection f_c is calculated through modelling the crack as a generalized plastic hinge. The two halves of the beam are both assumed to be rigid and rotate an angle θ:

$$\theta = \frac{\delta}{2\alpha h}. \tag{14}$$

Then the f_c can be estimated by:

$$f_c = \frac{L\theta}{2}k = \frac{\delta L}{4\alpha h}k \tag{15}$$

When k is a factor of uncracked part affecting the deflection caused by crack, it is estimated as:

$$k = \frac{\alpha}{0.9}, \quad 0 \le \alpha \le 0.9 \quad \text{and}$$

TABLE 1
Mix propositions of steel fibre concrete.

Cement	500 kg/m^3
Sand (maximum particle size 4 mm)	810 kg/m^3
Gravel (maximum particle size 8 mm)	810 kg/m^3
Superplasticizer (66% water content)	3.25 kg/m^3
Water	237.5 kg/m^3
Straight or hooked steel fibres	78.4 kg/m^3

$$k = 1, \quad 0.9 < \alpha \leq 1. \tag{16}$$

Experimental Verification

In order to verify the model, deformation-controlled three-point bending tests were carried out on two types of steel fibre concrete beams, straight fibre with circular cross-sections of 0.4 mm and 25 mm in length, and hooked fibre with circular cross-sections of 0.5 mm in diameter and 30 mm in length, here used separately. The size of beam was 420 × 100 × 100 mm and the span of bending was 400 mm. The concrete mixes are given in Table 1. Here the straight and hooked steel fibre concrete are abbreviated to SSFRC and HSFRC, respectively. The material parameters of Young's modulus E and tensile strength σ_t are determined directly from the uniaxial tensile test with dog-bone-shaped specimens (16) with the same mixes as used for beams. For the stress-crack width relationship, even though the micromechanics-based model described above provides a basic understanding of the influence of the micro-parameters on the shape of the stress-crack width curve, for structural application a more simplified model is needed. In this work, a four-linear model based on the directly measured stress-crack width ($\sigma - w$) data using both-side notched specimens with the same concrete mixes is used as input of $\sigma_I(x)$ in bending analysis. That is:

$$\frac{\sigma(w)}{\sigma_t} = a_i + c_i w \ (i = 1 \ldots 4). \tag{17}$$

The relative parameters a_i and c_i are listed in Table 2. The comparisons between predictions

TABLE 2
Material parameters used in four linear models for stress-crack width relationship.

Material parameters	SSFRC	W(mm)	HSFRC	W(mm)
E(GPa)	35	-	32	-
σ_t(MPa)	5.42	-	5.30	-
σ_c(MPa)	55.2	-	55.0	-
a_1,c_1(1/mm)	1,−9.96	0.00–0.03	1,−8.73	0.00–0.04
a_2,c_2(1/mm)	0.685,0.526	0.03–0.10	0.632,0.472	0.04–0.18
a_3,c_3(1/mm)	0.883,−1.45	0.10–0.38	0.8,−0.463	0.18–0.75
a_4,c_4(1/mm)	0.374,−0.11	0.38–2.00	0.532,−0.106	0.75–2.00

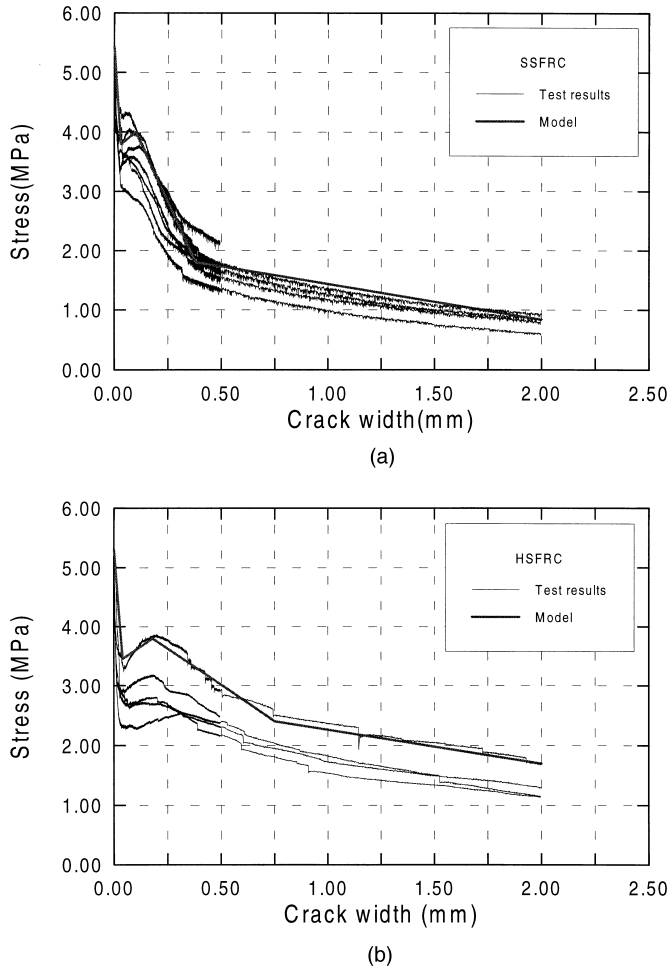

FIG. 2.
Measured stress-crack width data and four-linear model used in model and FE calculations, (*a*) SSFRC and (*b*) HSFRC.

of the simple model and the experimental data for these two types of FRC are shown in Figure 2. The details of test methods for determining stress-crack width relationship can be found elsewhere (5,10,12). Because the notches induce an uneven distribution of stress in the cracked section, normally the measured stress corresponding to a certain crack width is lower than the real value. Here a model by which the predictions are closed with the up boundary of test data is adopted.

The deflection is measured carefully during the testing, using a reference beam attached to the top of the beam by three steel blocks glued to the beam surface. Two standard Instron extensometers (type 2620–602) with 12.5 mm gauge length are used for measuring the deflection. The CMOD is measured by another extensometer with 50 mm gauge length mounted on the middle section of tensile side. Then, CMOD is equal to the measured deformation Δl minus the elastic deformation inside the gauge length. By assuming the stress

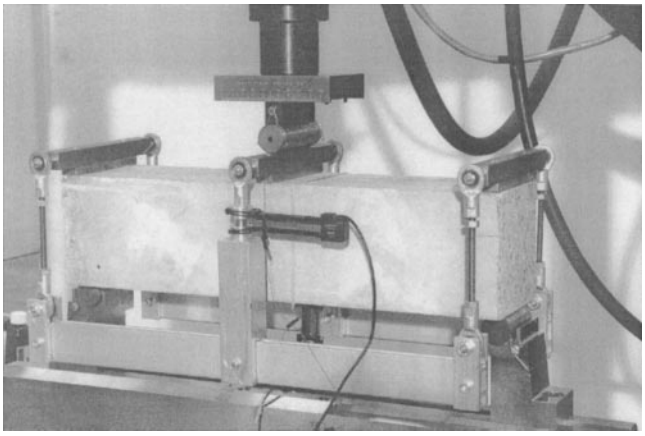

FIG. 3.
The experimental setup used for FRC beams in three-point bending.

in the gauge length is equal to the stress transferred by the crack, the CMOD can be given by:

$$\delta = \frac{\Delta l - a\Delta l_t}{1 + c\Delta l_t} \tag{18}$$

where a and c are given by the stress-crack width model shown in Eq. 16, l is the gauge length, and $\Delta l_t = \sigma_t l/E$. The experimental setup used for FRC beams in three-point bending is shown in Figure 3. The bending test is conducted as a prescribed deformation rate of 0.1 mm per minute, using the average signal from the two extensometers used for deflection measurement as feedback. All of the tests are carried out in a 250-KN capacity, 8500 Instron dynamic testing machine equipped for closed-loop testing.

Finite Element Implementation

The finite element method (FEM), as the most flexible and general numerical method, has been used and discussed extensively for fracture analysis of concrete (17–19). Fracture analysis of concrete by FEM can mainly be divided into two categories according to the concept of crack, i.e., discrete crack approach and smearch crack approach. The former approach models a crack as a geometrical discontinuity in which the performance after cracking can be described by stress-crack width relationship, and the latter imagines a cracked solid to be a continuum in which the performance after cracking can be described by stress-strain relation also. The discrete crack approach is used when the crack path is known in advance and along the interface between elements, such as in model I crack fracture. In the present work, the same beams with the same material characteristics are calculated by using a FEM program called DIANA, with discrete crack assumption. The beams are modelled using plain strain elements. In the analysis, the crack propagating path is assumed along the middle section of the beam and arranged to suit along element boundaries. Only half of the beam is modelled, and the fracture zone in the middle is modelled using non-linear spring elements. The load the spring can carry is evaluated through the stress-crack width (σ

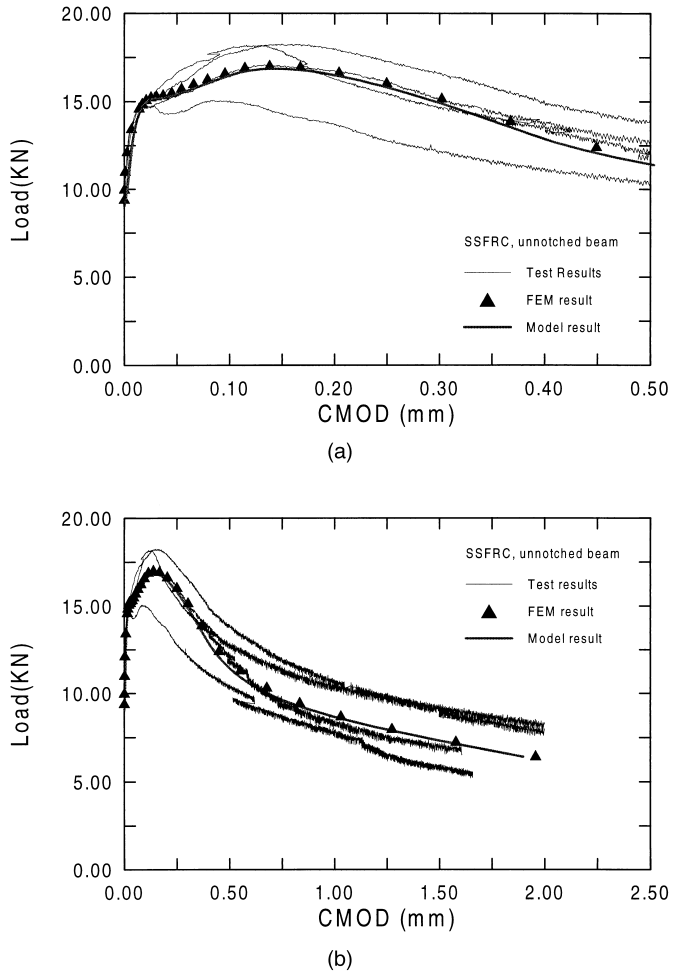

FIG. 4.
Comparison between model prediction, FEM calculation, and the experimental results in terms of load-CMOD curves of unnotched SSFRC beams, (*a*) 0–0.5 mm and (*b*) 0–2.5 mm.

$- w$) relationship. When the maximum principal tensile stress at the node point in front of the crack tip reaches the tensile strength of materials, this node will split into two nodes and a spring element is inserted. The crack tip moves to the next node.

Results and Discussion

In this section, the beams made of SSFRC and HSFRC, respectively, under three-point bending load are modelled. Results of the semi-analytical model are compared with the experimental results, as well as with the results of finite element analysis. The flexure performance steel fibre concrete is discussed.

In Figures 4 and 6, comparisons are shown between model predictions and experimental

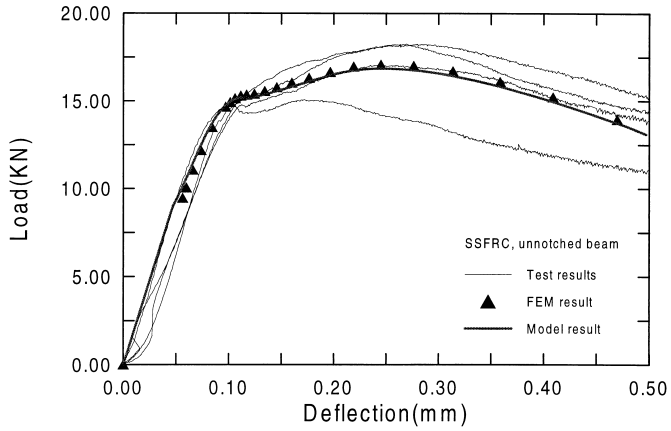

FIG. 5.
Comparison between model prediction, FEM calculation, and the experimental results in terms of load-deflection curves of unnotched SSFRC beams, (*a*) 0–0.5 mm and (*b*) 0–2.5 mm.

data, as well as finite element analysis results in terms of load-CMOD curves in the range of a) 0–0.5 mm and b) 0–2.5 mm. In Figures 5 and 7, predicted load-deflection curves according to Eqs. 11–15 are shown, along with experimentally determined curves as well as the finite element calculation in the range of 0–0.5 mm and 0–2.5 mm, respectively. Finally, Figure 8 shows the calculated relationship between load and crack length by present model and finite element method.

From Figures 4–7, it first follows that very good agreement can be obtained between present model-predicted and experimentally measured as well as finite element-calculated load-CMOD and load-deflection diagrams. The load-deflection curve can be divided into three sections: 1) elastic stage up to first crack load P_{fc} with a constant stiffness (dP/df); 2) crack developing period one, where load increases with a slow reduction of the stiffness of

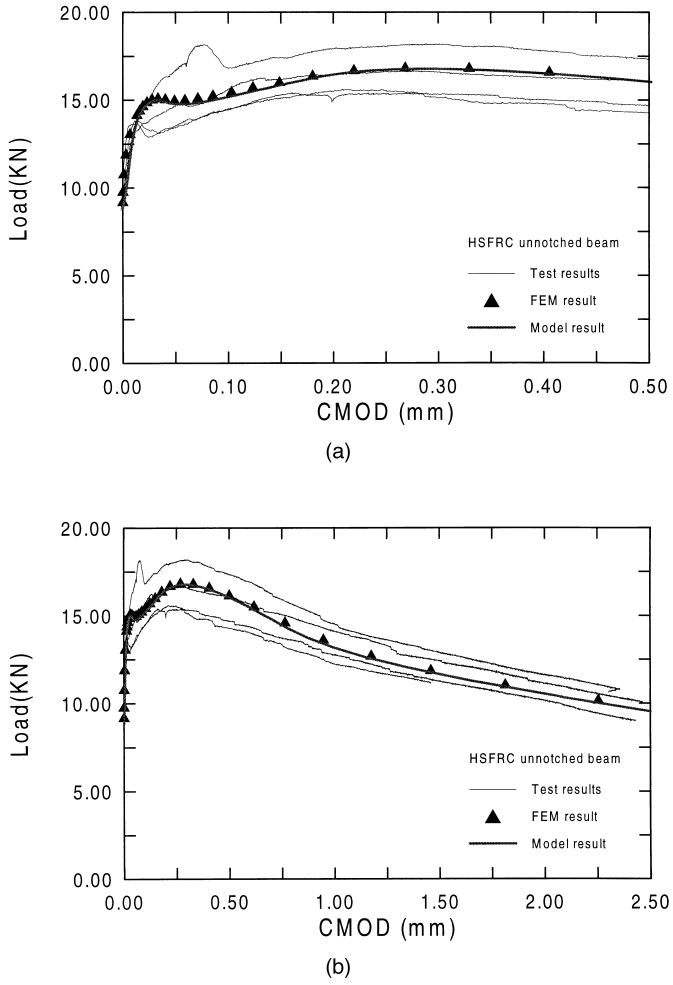

FIG. 6.
Comparison between model prediction, FEM calculation, and the experimental results in terms of load-CMOD curves of unnotched HSFRC beams, (*a*) 0–0.5 mm and (*b*) 0–2.5 mm.

beam until the crack length reaches about 40% of the beam depth; and 3) crack developing period two, where load increases with a significant reduction of stiffness until peak load at which stiffness becomes zero, after which load capacity starts to reduce with a negative stiffness.

In 1) and 2), the structural performance of SSFRC and HSFRC beams are almost identical. The load capacity will reach about 90% of its ultimate load with a limited deformation level, 0.025 mm and 0.12 mm for CMOD and deflection at the end of 2). In 3), load increases a little (10% of its ultimate load) with a significant increase in deformation. In this stage, the difference in load-deformation behaviour of SSFRC and HSFRC beams becomes pronounced. HSFRC beams can absorb more energy than SSFRC beams. In other words, the toughness of materials can be increased by the addition of hook-shaped fibre. From these

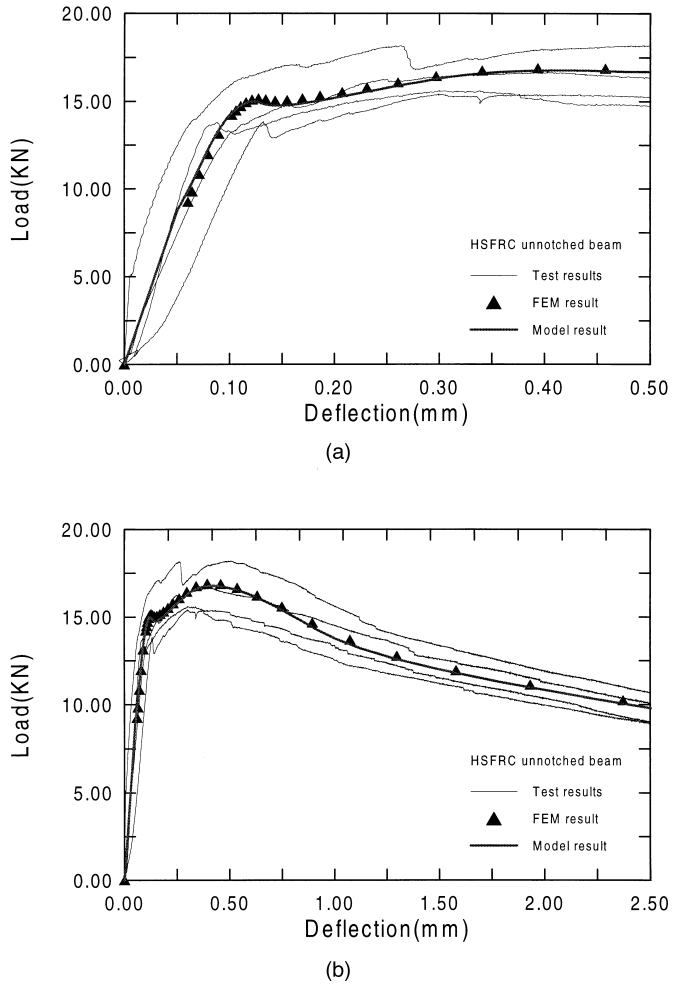

FIG. 7.
Comparison between model prediction, FEM calculation, and the experimental results in terms of load-deflection curves of unnotched HSFRC beams, (*a*) 0–0.5 mm and (*b*) 0–2.5 mm.

results, the CMOD, deflection and crack length at peak load of SSFRC and HSFRC beams are 0.15 mm, 0.25 mm, 0.8 h and 0.35 mm, 0.5 mm, 0.87 h, respectively. This also indicates that the shape of load-deflection or load-CMOD curves depends strongly on the shape of the stress-crack width curve. This shows us that in order to improve bending performance, the bridging behaviour of materials has to be improved first. As a fundamental material property of FRC, the bridging law is of notable significance in optimizing the structural properties of FRC structures, including the static performance such as tension and bending, as well as the cyclic performance such as impact and fatigue. It also can be found from the figures that the first crack load P_{fc} is close to half of the ultimate load of these two FRC beams. This is

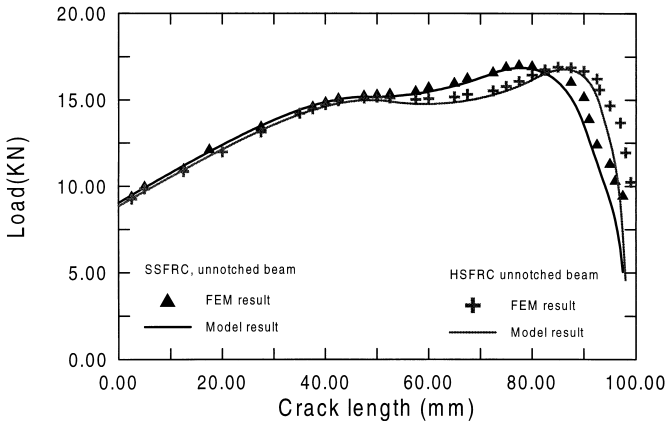

FIG. 8.
Relationship between load and crack length of FRC beam under three-point bending, model results, and FEM calculations.

because the process zone exists after cracking and causes the flexure strength to be higher than the tensile strength of materials as well as to be size-dependent.

At the same time, a defect of hooked fibre concrete compared with straight fibre concrete is also found. There is a load-dropping period before peak load with the increase of deflection, which can be seen in both experiments and modelling. This is due to the drop in the bridging stress after a crack (width 0 to 0.03 mm) appears (see Fig. 2). This shortcoming can be improved or overcome by optimizing the components of FRC materials, fibre geometry, and especially content.

Conclusions

A semi-analytical approach for modelling the flexure behaviour of FRC beams that relies on the stress-crack width relation as the fundamental constitutive relationship in tension has been presented. Very good agreement has been found between model predictions and experimental results as well as finite element calculations in terms of load-CMOD and load-deflection diagrams. This indicates that it is possible to obtain satisfactory predictions for complete structural performance in bending, such as load-CMOD and load-deflection responses with independently obtained experimental data for the stress-crack width relationship using present simple models. The important structural parameters for designers, such as bending toughness and ultimate load, as well as the corresponding deformation message, can easily be obtained through the present model.

From this model it can be deduced that the flexural performance is strongly dependent on the stress-crack width relation of materials. The optimum of bending behaviour of FRC structures can be achieved through optimizing the bridging behaviour of materials, finally leading to the modification of the bond characteristics of aggregate/matrix and fibre/matrix interfaces.

This model can be used to beam-type structures such as pavement overlays, bridge decks,

piles, and tunnel segments. Further work must be conducted to check its validity for larger specimens.

Acknowledgments

The work has been supported by a grant from the Danish Ministry of Education to the Technical University of Denmark. Jun Zhang would like to thank Dr. Hernik Stang for his valuable guidance during this work.

References

1. A. Hillerborg, M. Modéer, and P-E. Petersson, Cem. Concr. Res. 6, 773 (1976).
2. Z.P. Bazant and B.H. Oh, Mater. Struct. 16, 155 (1983).
3. J.P. Ulfkjær, S. Krenk, and R. Brincker, J. Engng. Mech. 121, 7 (1995).
4. C. Perdersen, Ph.D Thesis, Department of Structural Engineering and Materials, Technical University of Denmark, 1996.
5. H. Stang and T. Aarre, Cem. Concr. Compos. 14, 1432 (1992).
6. M. Maalej and V.C. Li, J. Mater. Civil Engng. 6, 390 (1994).
7. M. Maalej, V.C. Li, and T. Hashida, J. Engng. Mech. 121, 903 (1995).
8. V.C. Li, J. Mater. Civil Engng. 4, 41 (1992).
9. H. Stang, Report, Department of Structural Engineering and Materials, Technical University of Denmark, 1997.
10. J. Zhang and H. Stang, Proceedings of the Fifth International Symposium on Brittle Matrix Composites (BMC5), p. 43, Warsaw, Poland, 1997.
11. H. Stang and J. Zhang, Newpave Report, Department of Structural Engineering and Materials, Technical University of Denmark, 1994.
12. T. Aarre, Ph.D Thesis, Department of Structural Engineering and Materials, Technical University of Denmark, 1992.
13. V.C. Li, H. Stang and H. Krenchel, Mater. Struct. 26, 486 (1993).
14. H. Tada, The Stress Analysis of Cracks Handbook. Paris Prod. Inc., 1985.
15. S. Timoshenko, Strength of Materials, Part 1. Elementary Theory and Problems, 3rd edition, p, 174. D. Van Nostrand Company Inc., New York, 1955.
16. H. Stang, Newpave Report, Department of Structural Engineering and Materials, Technical University of Denmark, 1993.
17. M. Modéer, Report TVBM-1001, Division of Building Materials, University of Lund, Sweden, 1979.
18. P-E. Petersson, Report TVBM-1006, Division of Building Materials, Lund Institute of Technology, Sweden, 1981.
19. J.G. Rots, P. Nauta, G.M. Kusters, and J. Blaauwendraad, HERON 30, 1 (1985).